Hindered Diffusion of Polar Molecules Through and Effective Pore Radii Estimates of Intact and Ethanol Treated Human Epidermal Membrane

Kendall D. Peck,[1,2] Abdel-Halim Ghanem,[1] and William I. Higuchi[1]

Received February 2, 1994; accepted April 19, 1994

The *in vitro* passive transport of urea, mannitol, sucrose and raffinose across intact and ethanol treated human epidermal membrane was investigated. The intent of this study was to characterize the barrier properties and permeation pathways of these membranes for polar permeants under passive conditions. Based upon the relative permeabilities of these four solutes and hindered diffusion theory, the experimental data was adequately modeled for both membrane systems according to permeation through a porous membrane. Effective pore radii estimates for intact human epidermal membrane fell between 15 Å to 25 Å while similar estimates fell compactly between 15 Å to 20 Å for ethanol treated human epidermal membrane. Similarities between the relative permeabilities of human epidermal membrane for the four permeants studied and the relative permeabilities of these same permeants through ethanol pretreated human epidermal membrane indicate that significant similarities exist between the permeation pathways for both membrane systems. The results of this study have important implications for transdermal drug delivery in general and more specifically for strategies of designing effective chemical permeation enhancement systems.

KEY WORDS: human epidermal membrane; skin permeability; transdermal delivery; permeation enhancers; hindered diffusion; stratum corneum.

INTRODUCTION

It seems apparent that the first step in developing effective transdermal drug delivery systems is to characterize the barrier properties of human skin, due generally to the stratum corneum, which often inhibit the administration of effective doses of drug molecules into or through the skin. Despite numerous studies aimed at defining these barrier properties (1–4), the lack of a common consensus among pharmaceutical scientists regarding the nature of the pathway followed by molecules as they cross the human skin indicates that more basic research is needed in this area. Currently there are two schools of thought regarding the transport of molecules across skin. One consists of the view that the stratum corneum must be modeled in a dual nature as a membrane consisting of parallel porous and lipoidal pathways (4). The extent of the contribution of the specific pathway to the overall permeability is thought to be determined by the physicochemical parameters of the permeant molecule. Several investigators have viewed their data as being supportive of this model (4–6). On the other hand, some groups hold the view that the barrier properties of skin are adequately described by a lipoidal pathway (7). A substantial amount of data from a number of laboratories has been compiled and tested based upon this model, some of which is also viewed as evidence for the dual-pathway model, in an attempt to validate the single lipoidal pathway model. Although absolute characterization of the nature of the barrier properties of the human epidermal membrane (HEM) has remained somewhat elusive, the importance of such fundamental information may have far reaching implications for the future of transdermal drug delivery.

The transport enhancement of drug molecules across HEM, relative to passive transport across unaltered HEM, by means of chemical permeation enhancers and/or an applied electrical field seems imperative if effective doses are to be reached transdermally for many of the drugs which have been targeted for transdermal delivery. This is particularly true for peptides (8). However, development of effective enhancement systems should be based upon a fundamental understanding of the nature of the pathway being enhanced, as well as the effect of the enhancement mechanism upon this pathway during the delivery process. A great deal of recent research has in fact focused upon transport and barrier properties of skin under chemical enhancer conditions (6,9–11) as well as under an applied electrical field (12–16). The purpose of this study was to add to the current database regarding the nature of the permeation pathway for polar solutes through HEM and ethanol treated HEM under passive conditions. The passive permeation of four polar permeants (urea, mannitol, sucrose and raffinose) through HEM and ethanol treated HEM was studied and successfully modeled according to permeation through a porous membrane based upon hindered diffusion theory.

MATERIALS AND METHODS

Materials

Radio-labeled [^{14}C]urea, [^{3}H]mannitol, [^{14}C]sucrose and [^{3}H]raffinose of radiochemical purity ≥99% were obtained from New England Nuclear (Boston, MA). Absolute ethanol was obtained from U.S. Industrial Chemical Co. (Tuscola, IL). Human skin was obtained from Ohio Valley Tissue and Skin Bank (Cincinnati, OH). The epidermal membrane was removed by heat separation and immediately frozen for later use as previously described (13). Millipore® GSWP filters were obtained from Millipore Corp. (Bedford, MA). Polycarbonate membranes, with a nominal pore radius of 75 Å and porosity of 0.001, were obtained from Nuclepore Corp. (Pleasanton, CA). Phosphate-buffered saline (PBS), ionic strength 0.1 M, pH 7.5, was prepared from reagent grade chemicals and deionized water. All buffers also contained 0.02% sodium azide.

Mathematical Modeling

The general expression for the permeability coefficient of a molecule diffusing through a porous membrane is

[1] Department of Pharmaceutics and Pharmaceutical Chemistry, University of Utah, Salt Lake City, UT 84112.
[2] To whom correspondence should be addressed.

0724-8741/94/0900-1306$07.00/0

$$P = \frac{\epsilon D_r}{\tau h} \quad (1)$$

where P is the permeability coefficient, ϵ, τ and h are the porosity, tortuosity of the diffusional pathway and thickness of the membrane, respectively, and D_r is the diffusion coefficient of the permeant in the membrane. The parameters ϵ, τ and h characterize the properties of the membrane and can be grouped together into a membrane constant, C. D_r is a function of both the solute and membrane characteristics and can be expressed as the product of the free diffusion coefficient of the solute in solution, D, and the diffusional hindrance factor $F(\lambda)$ where λ is the ratio of the hydrodynamic radius of the solute, r, and the effective pore radius of the membrane, Rp (λ = r/Rp) (17). Making the appropriate substitutions into equation (1) yields

$$P = CDF(\lambda) \quad (2)$$

The hindrance factor is a well characterized function and has been reviewed in detail by Deen (17). In the instance where $\lambda \leq 0.4$, the hindrance factor can be expressed as

$$F(\lambda) = (1 - \lambda)^2[1 - 2.104\lambda + 2.09\lambda^3 - 0.95\lambda^5] \quad (3)$$

For membrane systems which are well characterized regarding the constants which are represented by C, equation (2) can be directly applied in estimating the effective pore radius of the membrane system (18). For the case of HEM permeation studies, C is an unknown thus making the direct application of equation (2) to obtain estimates of the effective Rp for HEM impractical. However, in the instance where permeability coefficients of multiple permeants are obtainable through the same HEM sample, C may be eliminated by taking the ratio of the permeability coefficients as follows

$$\frac{P_x}{P_y} = \frac{D_x F(\lambda_x)}{D_y F(\lambda_y)} \quad (4)$$

with the assumption that the pathway followed by the permeants is independent of the permeant molecule. The subscripts, x and y, in equation (4) correspond to the specific permeants. The ratio expressed as equation (4) is a function of the diffusion coefficients and the hydrodynamic radii of the permeants, which can be determined independently, and the effective pore radius of the membrane. By experimentally measuring the permeabilities of multiple permeants through the same membrane and substituting the appropriate solute parameters into equation (4), the effective pore radius of the membrane, Rp, can be determined by successive approximation. Hindered diffusion has been applied in a similar manner in the characterization of epithelial cell monolayer permeation pathways (19) and for ethanol pretreated HEM studies using polystyrene sulfonate permeants of various molecular weights (20).

Error Analysis

In an effort to obtain an indication of the reliability and stability of the mathematical calculations described in the mathematical modeling section, a simulated error analysis was conducted for the four permeants of interest. This error analysis involved first imagining an idealized membrane system with 22 Å pore radii. Based upon this hypothetical Rp and the appropriate physical parameters of the permeants, it was possible to calculate the relative idealized permeability coefficients for the four permeants such that any combination of these permeability coefficients substituted into equation (4) yielded a Rp of 22 Å. Once the relative values of the four idealized permeability coefficients were determined, hypothetical Rp estimates were made based upon holding three of the four permeability coefficients constant at the ideal values and varying one of the permeability coefficients by $\pm 10\%$ and $\pm 20\%$. This process was followed for each of the permeants in an effort to expose weakness in the calculation and understand the propagation of error from permeabilities to resulting Rp estimates.

Experimental Determination of Diffusion Coefficients

Custom made two-chamber side-by-side diffusion cells were used to determine the free diffusion coefficients used in the analysis of the permeation data. These cells were formed from Pyrex® tubes containing an embedded fritted glass disk (type-F, diameter 10 mm) (Corning, Newark, CA). The cells were constructed to have a 2.5 ml receiver chamber equipped with a stirring propeller, driven at 150 rpm, and a sampling port. The donor chamber was constructed such that after filling with solution it could be closed by means of a stopcock to prohibit any convective volume flow between the donor and receiver chambers. The donor solution, 2.5 ml volume, was stirred by a magnetic stir bar. Permeability coefficients for the fritted glass system are described by equation (2). The nominal pore size of the fritted glass is large ($\approx$5 μm) relative to the hydrodynamic radii of the permeants studied. Therefore, for the fritted glass system, the hindrance factor for diffusion is essentially unity and the permeability coefficient is proportional to the diffusion constant with C as the proportionality constant. The proportionality constant was determined for each of the fritted glass cells by calibration using sucrose, for which the diffusion coefficient at 37°C was taken from the literature (21), as the reference permeant. Diffusion coefficients were determined by experimentally obtaining permeability coefficients for the permeant of interest and solving for D based upon the permeant permeability and C for the fritted glass diffusion cells.

The actual permeability experiments were conducted by placing 2.5 ml of PBS in the receiver chamber and 2.5 ml PBS, premixed with the radio-labeled, tracer-level, permeant in the donor chamber. All solutions were warmed to 37°C before starting the experiment and the experiments were maintained at 37°C by a circulating waterbath. Receiver samples were withdrawn after appropriate time intervals, sample volumes were replaced with PBS after each sample. The donor solution was sampled immediately before and after the permeability experiments. Permeability coefficients were then calculated according to

$$P = \frac{1}{AC_D}\frac{dQ}{dt} \quad (5)$$

where A is the diffusional area of the membrane (0.785 cm^2), C_D is the donor concentration and (dQ/dt) is the slope of the

linear region of the amount of permeant in the receiver chamber versus time plot. Receiver and donor samples were assayed by liquid scintillation counting as described below.

HEM Permeability Experiments

The basic HEM permeability protocol followed in this study has been outlined in detail previously (22). Important aspects of this protocol will be reviewed briefly. Electrical resistance of the HEM was used as a primary selection criterion (≥ 15 kΩcm^2) and to monitor the HEM stability during the experimental period. The HEM was supported in the diffusion cells by a Millipore® GSWP filter to minimize damage resulting from physical stresses placed upon the HEM during the protocol. HEM has been shown to be stable with respect to mannitol permeability and electrical resistance under these conditions for five days (22). All permeability experiments were conducted in 0.1 M PBS. Dual-permeant experiments were conducted to allow two permeability coefficients to be determined per permeability experiment. This increased the amount of data which could be collected for each HEM sample. The permeant pairs used were [^{14}C]urea with [^{3}H]mannitol and [^{14}C]sucrose with [^{3}H]raffinose. Performing successive permeability experiments allowed permeability coefficients for each permeant to be determined for each HEM sample. The protocol involved sampling and replacing the total receiver volume four times over a 12 hour period and calculating the experimental permeability coefficient according to equation (5). Tracer-level donor concentrations insured that osmotic pressure did not contribute to the resulting permeability coefficients. All samples were mixed with 10 ml scintillation cocktail (Ultima Gold™, Packard, Meriden, CT) and assayed for each permeant by dual-labeled liquid scintillation counting using a Packard Tri-Carb™ 2500TR Liquid Scintillation Analyzer. The instrument was calibrated to account for the differences in quenching between the ^{3}H and ^{14}C isotopes.

There were three general protocols followed: two-day, three-day and five-day. The two-day protocol consisted of determining the permeabilities of urea and mannitol on day one and the permeabilities of sucrose and raffinose on day two for each HEM sample. For the three-day protocol, the permeabilities of urea and mannitol were determined on day one and again on day three while the permeabilities of sucrose and raffinose were determined on day two. The five-day protocol was an extension of the shorter protocols with urea and mannitol permeabilities being determined on days one, three and five while the permeabilities of sucrose and raffinose were determined on days two and four. There are six unique permeability coefficient ratios (Pm/Pu, Ps/Pu, Pr/Pu, Ps/Pm, Pr/Pm, Pr/Ps) obtainable from pairs of the four permeability coefficients of urea, mannitol, sucrose and raffinose (designated as Pu, Pm, Ps and Pr respectively). Therefore six Rp estimates can potentially be determined from a two-day protocol through equation (4) if all possible ratios are considered. If all possible ratios are considered for a three-day protocol, thirteen total Rp estimates may be obtained: four from combinations of the Pu and Pm values, two each from the following ratio types: Ps/Pu, Pr/Pu, Ps/Pm, Pr/Pm; and one Rp estimate may result from the Pr/Ps ratio. Ideal results from a five-day protocol would yield 37 Rp estimates.

The protocols for which the permeability coefficients of a permeant pair were determined more than once are particularly suited for studies of this nature. Each HEM sample served as its own control in this study in an attempt to gain quantitative data by eliminating the difficulties which result from skin-to-skin variability (23). The underlying premise behind this approach is that the barrier properties of the HEM must remain constant during the entire period of the protocol. Based upon the experimental protocol as it has been designed, any changes in the barrier properties of the HEM can be readily detected based upon both significant changes in permeability for a particular solute over successive permeability experiments and changes in electrical resistance (22).

Ethanol Pretreated HEM Permeability Studies

Permeation studies were also conducted with HEM which had been exposed to a two-hour pretreatment with ethanol. The pretreatment protocol involved cell setup and equilibration as previously described (22) followed by thoroughly rinsing the cell in absolute ethanol and maintaining the cell with ethanol in both chambers at 37°C for two hours. Following pretreatment, the cell was thoroughly rinsed with PBS and allowed to equilibrate in PBS for 24 hours before starting the permeation experiments. Two sets of ethanol pretreated HEM experiments were conducted: one following the two-day protocol and one following the three-day protocol, both protocols have been described above. The permeability experiments were conducted over a 3–4 hour period.

Nuclepore® Permeation Studies

Permeation studies with the same four permeants were also conducted with a Nuclepore® membrane system. The diffusion cells were the same as those used in the HEM studies. The membrane was composed of a stack of 20 individual membranes sandwiched between the half-cells of the diffusion cell. Similar systems have been used in previous studies (24). Dual-labeled experiments were conducted with the samples being assayed as described above.

RESULTS

Experimentally Determined Diffusion Coefficients

The experimentally determined diffusion coefficients obtained from the fritted glass permeability experiments are shown in Table I along with corresponding values used by Beck and Schultz in a related study with these permeants (18). The values reported by Beck and Schultz were determined at 25°C, thus for comparative purposes these values were extrapolated to 37°C based upon temperature and viscosity changes. As can be seen in Table I, general agreement is good between the extrapolated values taken from Beck and Schultz and the values determined experimentally. The values for the diffusion coefficients are the averages of five experiments for each permeant, in each case the relative standard deviation was <3.5%. The diffusion coefficients were determined relative to the diffusion coefficient of sucrose which was experimentally found to be 6.98×10^{-6} cm^2/s at 37°C by Deen et al. (21). The permeant radii shown

Table I. Permeant Physical Parameters

Permeant	D * $10^{6a,b}$ cm^2/s	r_s(Å)[a]	D* 10^6 cm^2/s	r_s(Å)
^{14}C-urea	18.5	2.64	17.5 ± 0.4[c]	2.73
^{3}H-mannitol	9.14	4.33	9.03 ± 0.3[c]	4.44
^{14}C-sucrose	6.98	5.55	6.98 ± 0.2[d]	5.55
^{3}H-raffinose	5.81	6.54	5.72 ± 0.1[c]	6.62

[a] Taken from reference 18.
[b] Corrected for temperature and viscosity from 25°C to 37°C.
[c] Average ± standard deviation, n = 5.
[d] Taken from reference 21.

in Table I are based upon the Stokes-Einstein radii, calculated for each permeant from its diffusion coefficient, corrected by the factor proposed by Gierer and Wirtz (25). This process is identical to that followed by Beck and Schultz (18).

Error Analysis

The results of the simulated error analysis are shown in Figs 1 and 2. Fig. 1 shows the results of varying the permeability of urea while holding the permeabilities of mannitol, sucrose and raffinose constant. Fig. 2 shows the results of varying sucrose permeability while holding the permeabilities of the other permeants constant. The ratios shown on these figures (i.e. Px/Py) indicate the ratio used in equation (4) to make the Rp estimates represented by the points on the figures. The x-axis of these figures correspond to the number of Rp estimates which result from unique permeability coefficient ratios. Some important practical considerations resulted from this analysis. First, the Rp variability which results from varying the permeability coefficients is not symmetric about the ideal Rp value of 22 Å and is dependent upon the direction which the permeability is varied. It should be noted that the Rp variability is suppressed when the variability results in Rp estimates less than 22 Å and expanded when the variability results in Rp estimates greater than 22 Å. Experimentally, random error in the permeability coefficients will result in the arithmetic mean of the Rp estimates being biased in the positive direction. Second, the magnitude of the variation of the resulting Rp estimates is also dependent upon the relative radii and diffusion coefficients of the permeants used to make the Rp estimates. This is most evident by observing the Rp estimates in Fig. 2, which result from the combination of the varied sucrose permeability coefficient with the ideal mannitol and raffinose permeability coefficients. When sucrose is varied by −20% the Pr/Ps ratio results in an Rp estimate which is off-scale on Fig. 2 due to the diffusivities of sucrose and raffinose differing only by approximately 20%.

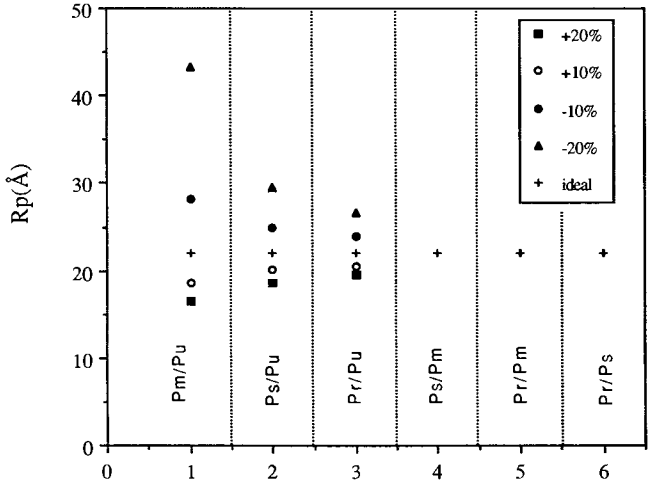

Fig. 1. Resulting simulated Rp estimates when the urea permeability coefficient is varied while holding the other permeability coefficients constant.

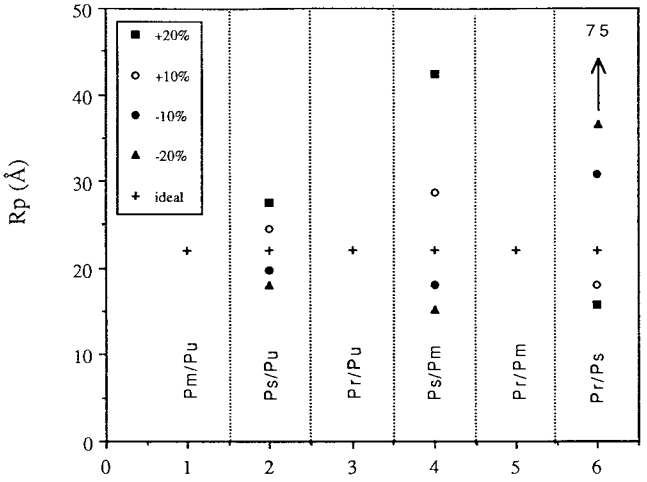

Fig. 2. Resulting simulated Rp estimates when the sucrose permeability coefficient is varied while holding the other permeability coefficients constant.

From a strictly mathematical standpoint, the overall technique, as it has been applied, is most limited by experimental variability in cases where the diffusivities of the permeants are similar. Based upon these observations, the most reliable Rp estimates are then expected to result from permeability coefficient ratios resulting from the permeants which differ to the greatest degree in size. For this reason, the greatest weight will be given to Rp estimates which result from permeability ratios which involve urea as the reference permeant (used as the denominator of equation (4)) relative to raffinose, sucrose and mannitol. The permeability of "unaltered" HEM to these polar solutes is inherently low making it difficult to determine accurate permeability coefficients, particularly for raffinose and sucrose. Based upon the error analysis, significant variability in the experimental HEM Rp estimates was anticipated.

HEM Permeation Experiments

The permeability coefficients resulting from the permeation studies with HEM are shown in Table II. The first five experiments followed the two-day protocol and the last six were five-day protocols. Table II also shows the electrical resistance measurements of the HEM samples for each experiment; the specific resistance values are the averages of the measurements taken immediately before and after the permeation experiments. The permeability coefficient data of day one for experiment 8 and day five for experiment 10

Table II. HEM Permeability Coefficients and Electrical Resistance Measurements

	Permeability * 10^8 (cm/s)										Resistance (kΩ * cm²)				
	Day 1		Day 2		Day 3		Day 4		Day 5						
Exp. #	Pu	Pm	Ps	Pr	Pu	Pm	Ps	Pr	Pu	Pm	Day 1	Day 2	Day 3	Day 4	Day 5
1	1.88	0.64	0.40	0.22							94	94			
2	2.80	1.11	0.62	0.45							72	75			
3	1.84	0.44	0.22	0.12							92	92			
4	35.4	12.3	5.83	4.32							16	17			
5	10.3	3.51	1.71	1.29							38	39			
6	1.65	0.35	0.28	0.17	1.44	0.38	0.29	0.19	1.52	0.41	107	128	122	131	134
7	4.21	1.38	0.79	0.63	5.23	1.46	0.84	0.65	4.73	1.31	63	63	54	56	58
8			0.85	0.63	6.71	2.30	0.92	0.53	6.32	2.04	114	116	114	112	114
9	1.43	0.49	0.23	0.18	1.43	0.55	0.27	0.19	1.44	0.53	149	148	165	161	165
10	1.42	0.22	0.18	0.12	1.32	0.26	0.16	0.11			118	117	126	133	107
11	3.79	1.04	0.36	0.41	3.39	0.96	0.36	0.32	3.08	0.87	72	75	76	84	86

have been excluded from the Rp calculations. The experimentally determined mannitol permeability coefficients determined for these two days were significantly higher than the mannitol permeability coefficients determined over the course of the respective protocols. For this reason days 2–5 were included in the Rp calculations for experiment 8 and days 1–4 were used in the calculations for experiment 10. Figs 3 and 4 show representative Rp estimates which result from the permeability data in Table II and the application of equation (4). Fig. 3 shows the Rp estimates which result from the permeability coefficients determined in experiment 1. Fig. 4 shows the resulting Rp estimates from experiment 9. As for Figs 1 and 2, the x-axes of Figs 3 and 4 correspond to the number of potential Rp estimates resulting from the specific experimental protocols which the figures represent. Table IV shows a summary of the Rp estimates for all of the HEM experiments. The Rp averages and standard deviations shown are based upon all of the Rp estimates for a particular experiment which resulted from urea based permeability ratios (i.e. Pm/Pu, Ps/Pu and Pr/Pu). The effective pore radii estimates for these HEM samples fall consistently between 15 Å to 25 Å with only one HEM sample giving results outside this range.

Ethanol Pretreated HEM Permeation Studies

The resulting permeability coefficients for ethanol pretreated HEM are shown in Table III accompanied by the corresponding electrical resistances of each HEM sample before ethanol treatment and during the permeation protocols. Fig. 5 shows a representative example of Rp estimates resulting from the permeability coefficients of experiment 8e. The Rp estimates for ethanol treated HEM are remarkably constant and independent of the permeability coefficient ratio used to obtain the estimate. This constancy, as opposed to the greater variability seen for "unaltered" HEM, is most likely due to the increase in permeability (approximately 100-fold relative to untreated HEM) resulting from ethanol treatment which decreases the experimental error and uncertainty of the permeability coefficients. Table IV includes a summary of the Rp estimates for all of the

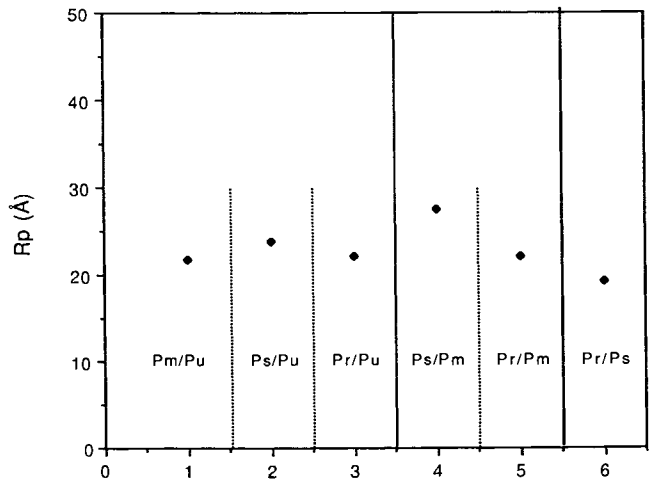

Fig. 3. Representative results of a two-day HEM protocol. The ratio from which each Rp estimate originated is indicated and the x-axis corresponds to the number of estimates which result from the two-day protocol.

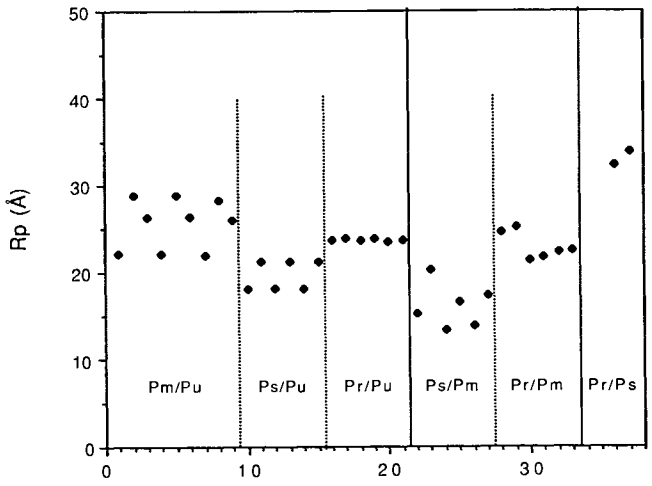

Fig. 4. Results of the five-day HEM protocol corresponding to experiment #9 in Tables II and IV. The ratio type from which each Rp estimate originated is indicated and the x-axis corresponds to the number of estimates which result from the five-day protocol.

Table III. Ethanol Pretreated HEM Permeability Coefficients and Electrical Resistance Measurements

	Permeability * 10^6 (cm/s)									
	Day 1		Day 2		Day 3		Resistance (kΩ * cm^2)			
Exp. #	Pu	Pm	Ps	Pr	Pu	Pm	Before EtOH	Day 1	Day 2	Day 3
1e	25.1	8.60	5.30	3.20			87	0.18	0.16	
2e	3.12	0.98	0.45	0.26			153	1.18	1.20	
3e	3.57	1.06	0.55	0.33			32	0.87	0.89	
4e	5.41	1.83	0.95	0.55			27	0.62	0.67	
5e	4.65	1.51	0.68	0.41			26	0.77	0.81	
6e	1.82	0.47	0.22	0.12			240	1.85	1.90	
7e	2.38	0.74	0.28	0.15	2.53	0.74	127	1.30	1.30	1.30
8e	5.82	1.78	0.80	0.40	5.46	1.66	61	0.60	0.80	0.60
9e	4.35	1.26	0.54	0.26	4.84	1.45	73	0.75	0.90	0.40
10e	6.77	2.24	1.06	0.55	6.13	1.84	17	0.35	0.40	0.35
11e	13.2	3.92	2.18	1.12	13.8	4.30	39	0.16	0.19	0.14

ethanol pretreated HEM samples. In Table IV, no Rp estimates have been excluded from the averages shown (Rp's from all possible permeability coefficient ratios for ethanol pretreated HEM have been included). The effective pore radii for ethanol pretreated HEM fall between 15 Å to 25 Å and more compactly between 15 Å to 20 Å.

Nuclepore® Permeation Studies

Studies conducted with the synthetic Nuclepore® membranes were done as a check of both the experimental technique and the physical parameters determined for the permeants. The results of these experiments are summarized by Fig. 6. Fig. 6 also summarizes the results from the fritted glass, two-day protocol HEM and two-day protocol ethanol treated HEM experiments. In Fig. 6, the average of the permeability coefficients normalized by the permeability of urea for each individual experiment are plotted versus the permeant radii of the numerator permeant. The choice of the x-axis is arbitrary in this case and was chosen for convenience. The lines superimposed upon the experimental data points are the permeability ratios calculated from equation (4) using the Rp value shown in the legend and the appropriate permeant parameters from Table I. There is obvious excellent agreement between the experimentally determined data points and the theoretically calculated ratios based upon a Rp of 80 Å for the Nuclepore® data. The nominal pore radius for these membranes according to the manufacturer is 75 Å. Due to the relatively small sizes of the permeants used in this study, the sensitivity of this technique is expected to be quite low in the pore size range of the Nuclepore® membrane. In fact, the modest error indicated by the standard deviation of the ratios shown for Nuclepore® data in Fig. 6 correspond to a Rp range of 65 Å to 110 Å. With these points in mind, the Nuclepore® data serves to give strong support to the technique as it has been applied in this study and thus the Rp estimates obtained for HEM. The Rp estimates obtained for HEM are in the range, based upon the permeants used in this study, for which this technique should have its greatest sensitivity (i.e. significant hindrance while the ratio of permeant radius to pore radius is well below the limit of $\lambda \leq 0.4$). This is born out by the relative

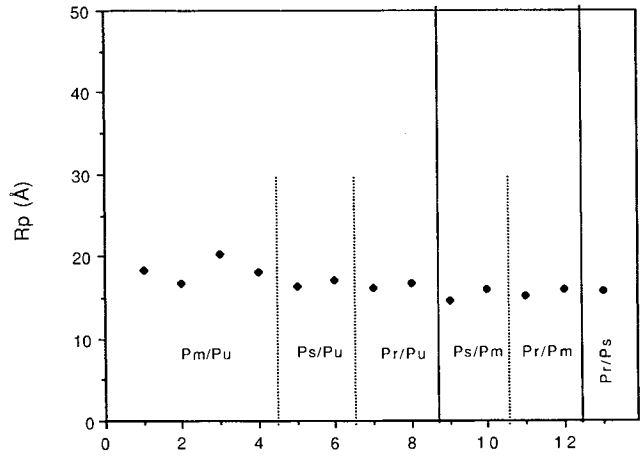

Fig. 5. Representative results of a three-day ethanol pretreated HEM protocol. The ratio type from which each Rp estimate originated is indicated and the x-axis corresponds to the number of estimates which result from the three-day protocol.

Table IV. Rp Estimate Summary

HEM Rp Estimates[a]			EtOH HEM Rp Estimates[c]		
Exp. #	# of Estimates	Rp (Å)[b]	Exp. #	# of Estimates	Rp (Å)
1	3	23 ± 1	1e	6	24 ± 2
2	3	29 ± 3	2e	6	17.6 ± 1.8
3	3	15 ± 1	3e	6	18.7 ± 1.5
4	3	21 ± 2	4e	6	19.8 ± 1.3
5	3	21 ± 2	5e	6	18 ± 3
6	21	18 ± 5	6e	6	16.2 ± 1.8
7	21	19 ± 5	7e	13	16 ± 2
8	12	19 ± 3	8e	13	16.5 ± 1.8
9	21	23 ± 3	9e	13	15 ± 2
10	12	15 ± 3	10e	13	19 ± 3
11	21	17 ± 3	11e	13	18.1 ± 1.2

[a] Results from intact HEM.
[b] Average ± standard deviation based upon Pm/Pu, Ps/Pu and Pr/Pu ratios.
[c] Results from ethanol pretreated HEM.

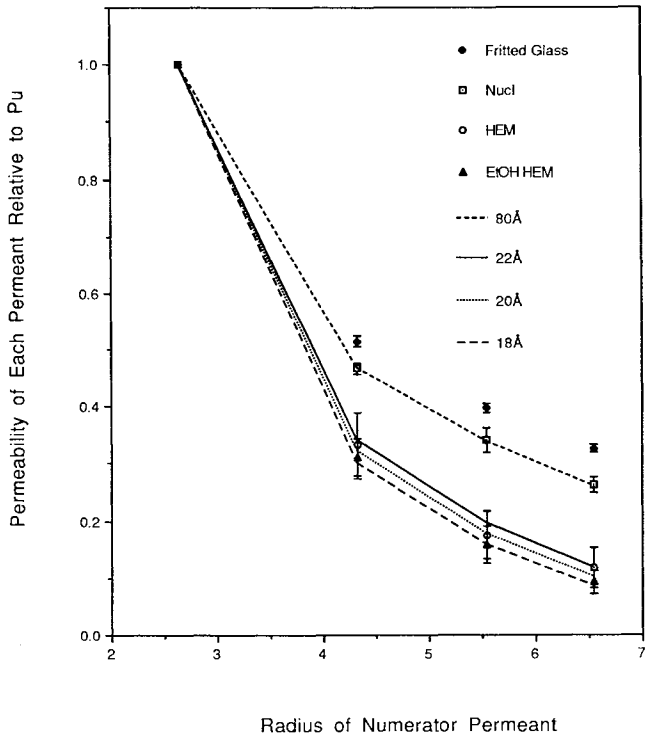

Fig. 6. Relative effect of hindrance for the four membrane systems studied. The superimposed lines correspond to calculated results based upon Eq. (4) and the Rp indicated in the legend.

effect of hindrance evident from the differences in the permeability ratios for the membrane systems included in Fig. 6.

DISCUSSION

The overall results from untreated HEM give a strong indication that the membrane barrier properties to the permeants studied correlate with a porous membrane with effective pore radii of 15 Å to 25 Å. This view directly contrasts the concept of the membrane being adequately characterized strictly as lipoidal in nature. Potts and Guy (7) have recently proposed a correlation, based upon the concept of a lipid pathway, intended to allow predictions of HEM permeability for solutes based upon the octanol/water partition coefficient (K_{oct}) and molecular weight of the solute. Using equation (7) of reference 7 and $\log K_{oct}$ values taken from reference (26), it is possible to "predict" the permeability of the solutes used for this study and compare those predicted values with the experimental data of this study. The results of this analysis, which are summarized in Table V, conclusively show that the data obtained in this study cannot be accounted for by arguments given in reference 7. First, the correlation proposed in reference 7 underestimates the permeability of each permeant by a factor ranging from one order of magnitude for urea to over three orders of magnitude for raffinose as shown by the final column of Table V. Secondly, there is approximately one order of magnitude difference between the urea and raffinose permeabilities for individual HEM samples shown in Table II (and the corresponding average values shown in Table V). The correlation proposed by Potts and Guy predicts this difference to be

Table V. Comparison of Lipoidal Model vs. Experiment

Permeant	MW	$\log K_{oct}$	Predicted $\log P^d$	Observed $\log P^e$	Observed P / Predicted P
urea	60.1	−2.75[a]	−8.62	−7.45	15
mannitol	182.2	−3.10[b]	−9.60	−7.94	45
sucrose	342.3	−3.67[b]	−11.0	−8.24	560
raffinose	504.4	−3.67[c]	−12.0	−8.37	4100

[a] Average of five values reported in reference 26.
[b] Taken from reference 26.
[c] No $\text{Log}K_{oct}$ was given in reference 26 for raffinose therefore the value reported for sucrose was used as an approximate value and should be viewed as an upper limit for raffinose.
[d] Predicted based upon equation (7) in reference 7.
[e] Averages of the average values obtained for each experiment listed in Table II. Experiment 4 was not included as it seems to be an outlier. Had it been included the ratios reported in the final column would have been greater.

greater than three orders of magnitude. These comparisons have been made to emphasize the fact that data which gives a reasonable fit to the proposed pore model, as does the permeation data obtained in this study, cannot be accounted for by the correlation proposed in reference 7. It is equally straight-forward to show that the permeation characteristics of lipophilic compounds cannot be accounted for by the proposed pore model.

Some may question the existence of a pore pathway in light of the high measured apparent activation energy for water transport across skin (≈15–20 kcal/mol), relative to the apparent activation energy of bulk diffusion (≈5 kcal/mol). The permeability of uncharged solutes across lipid bilayer membranes has been shown to be a function of the physicochemical properties of the solute (27). The proposed exponential dependence of permeability upon molecular volume makes the size of the solute a critical parameter for bilayer permeability. Due in part to a small molecular volume, water crosses many lipid bilayers much more readily than other polar molecules such as urea (27), and the measured apparent activation energy for water diffusion across skin may be due to temperature induced changes in the lipid regions of the skin as some have proposed (28). This, however, does not rule out the possibility of water diffusing through a parallel porous pathway. It is probable that the effective fractional area of any pores in the stratum corneum is extremely small relative to the fractional area of the lipoidal pathway. As water is known to penetrate lipid membranes, it is likely that significant water transport occurs via the lipid regions of the HEM. Also, when one measures a single apparent activation energy for simultaneous processes of comparable importance but which have different activation energies, such as diffusion through parallel pathways, the apparent activation energy may be weighted heavily by the activation energy of the more temperature dependent process. Water may diffuse through the porous pathway as expected based upon the proposed model; however this mechanism may not be apparent based upon temperature dependence studies. Evidence which confirms these views comes from the measured apparent activation energy of transport for ions (10) and the polar molecules of this study (unpublished results from our laboratory) through skin. In both cases, these measured val-

ues are close to the activation energies of bulk diffusion in water (≈5 kcal/mol) which is consistent with transport through a porous pathway.

The experiments in this study were designed to obtain information regarding the general barrier properties of the HEM for polar solutes rather than to correlate the permeation pathway to specific sites in the HEM. It has been suggested that appendages provide the transdermal passive penetration pathway for ions (10). However, a recent study (22) has shown that the ionic strength dependent permeability of the tetraethylammonium ion is not consistent with an effective pore size equivalent to the lumen of common shunts (i.e. sweat glands, hair follicles, etc.) under physiological conditions. Likewise, the effective pore radii which have been estimated in this study are much smaller than shunts in normal skin. Even under skin altering iontophoretic conditions, for which appendages have been shown to contribute significantly to the conduction of current through skin (29), experimental data from hairless mouse skin (16) and hairless rat skin (12) has led to effective pore radius estimates in the range of 20 Å. These observations are made simply to discourage the assumption that the dimensions of porous permeation pathways through skin should correspond to dimensions of sweat glands and other appendages in normal, unhydrated skin. However, we emphasize that these observation do not eliminate the possibility that appendages may function as a significant, or even dominant, permeation route for these polar solutes through HEM as: 1) the observed hindrance may result from the dimensions of the appendages being restricted under experimental conditions due to hydration induced swelling of the HEM; and 2) the rate limiting barrier to diffusion through such appendages may be localized at the epithelial cell layers lining the appendages, as described by Kasting and Bowman (30), rather than diffusion through the lumen of the appendages. Although information has been obtained regarding the effective pore radii for the HEM samples studied when the diffusion is modeled according to a porous pathway model, additional work is necessary to correlate this data to specific morphological or structural properties of the HEM.

Another consideration which has not been discussed to this point is the distribution of pore sizes which may exist in HEM. It is conceivably possible to model the data according to a bi- or tri-pore size distribution. Such modeling would be possible if specific trends had been generally observed with respect to specific permeant permeability ratios (which would translate into permeant dependent trends in the Rp estimates). As no general trends were observed for the HEM data (see Figs 3 and 4), no such attempts were made to fit the data to a pore-size distribution model. To make such calculations meaningful, it would be necessary to obtain permeation data for many permeants spanning a larger molecular size range, low permeabilities and skin-to-skin variability for intact HEM make such experiments impractical.

One of the most notable outcomes of the ethanol treated HEM studies is that, despite decreasing the electrical resistance of HEM by approximately two orders of magnitude, the resulting effective pore radii estimates are approximately the same as those determined for intact HEM. This conclusion indicates that extraction of HEM lipids by ethanol pretreatment greatly increases porosity while creating pores with effective radii which are quite small. The implications of this result are meaningful in the effort to enhance transdermal delivery of drug molecules in the molecular size range of many therapeutic peptides. For such molecules, the effect of hindrance for diffusion through an effective pore with a radius in the range of ≈20 Å is significant. An ideal enhancement scenario would be to increase porosity coupled with an increase in effective pore size. This concept is illustrated by Fig. 7. Fig. 7 shows the estimated effect of increasing the effective pore radius of a membrane, while maintaining constant porosity, upon the permeability of peptides/proteins in the molecular weight range of 1200 to 10,000. The protein parameters used to make the calculations represented by Fig. 7 were estimated from diffusion coefficient and size data for peptides and proteins. As can be seen from Fig. 7, doubling the effective pore radius from 20 Å to 40 Å is estimated to result in permeability increases of 3, 10 and 25-fold for peptides/proteins of 1200, 5000 and 10,000 molecular weight. If one added an increase in porosity of 100-fold, as is observed for ethanol treated HEM, the corresponding enhancement factors resulting from increased porosity and decreased hindrance would be 300, 1000 and 2500 for the three molecular weights considered. Ongoing experiments in our laboratories are aimed at obtaining a mechanistic understanding of different classes of penetration enhancers in an effort to achieve a system capable of facilitating delivery of peptides/proteins.

CONCLUSION

The results of this study have led to the estimation of the effective pore radii of HEM and ethanol treated HEM. Although a porous pathway model has been hypothesized for quite some time to account for HEM permeation data, this is the first time physical parameters such as effective pore size have been estimated for intact HEM. The results of this study will serve as a useful baseline to which HEM under chemical permeation enhancement conditions and/or an applied electrical field may be compared. The similarities be-

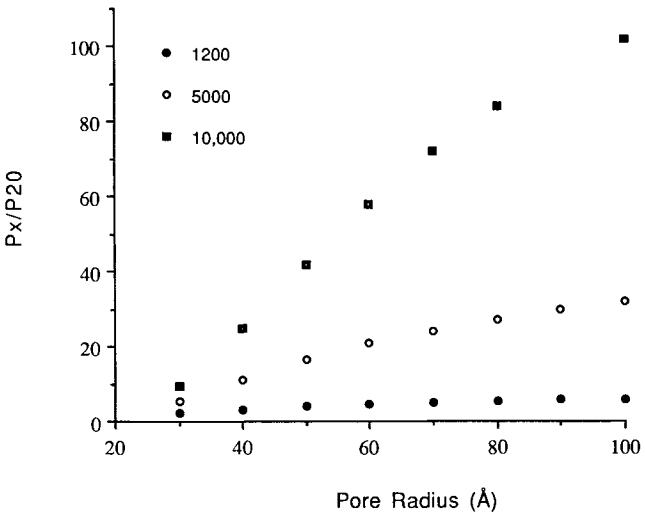

Fig. 7. Hypothetical permeability enhancement for three different molecular weight proteins resulting from increasing the effective Rp relative to 20 Å while holding porosity constant.

tween the permeation data obtained from HEM and ethanol treated HEM using the polar permeants of this study indicate that the permeation pathways for these two membrane systems are closely related with membrane porosity accounting largely for the difference in permeability. Finally, effective transdermal permeation enhancement for peptide/protein drugs may rely upon obtaining means of expanding the effective pore radii as well as porosity of the HEM.

ACKNOWLEDGMENTS

This research has been funded by NIH Grant GM43181 and an American Foundation for Pharmaceutical Education Predoctoral Fellowship. The authors wish to thank TheraTech Inc., Salt Lake City, UT for supplying the skin samples for this study.

REFERENCES

1. R. J. Scheuplein and I. H. Blank. Permeability of skin. *Physiol. Rev.* **51**:702–747 (1971).
2. A. S. Michaels, S. K. Chandrasekaran, and J. E. Shaw. Drug permeation through human skin: Theory and in vitro experimental measurement. *AIChE J.* **21**:985–996 (1975).
3. P. V. Raykar, M. C. Fung, and B. D. Anderson. The role of protein and lipid domains in the uptake of solutes by human stratum corneum. *Pharm. Res.* **5**:140–150 (1988).
4. T. Hatanaka, M. Shimoyama, K. Sugibayashi, and Y. Morimoto. Effect of vehicle on the skin permeability of drugs: Polyethylene glycol 400-water and ethanol-water binary solvents. *J. Controlled Release* **23**:247–260 (1993).
5. C. Ackermann, G. L. Flynn, and W. M. Smith. Ether-water partitioning and permeability through nude mouse skin in vitro. II. Hydrocortisone 21-*n*-alkyl esters, alkanols and hydrophilic compounds. *Int. J. Pharm.* **36**:67–71 (1987).
6. Y. H. Kim, A. H. Ghanem, H. Mahmoud, and W. I. Higuchi. Short chain alkanols as transport enhancers for lipophilic and polar/ionic permeants in hairless mouse skin: Mechanism(s) of action. *Int. J. Pharm.* **80**:17–31 (1992).
7. R. O. Potts and R. H. Guy. Predicting skin permeability. *Pharm. Res.* **9**:663–669 (1992).
8. V. Srinivasan, W. I. Higuchi, S. M. Sims, A. H. Ghanem, and C. R. Behl. Transdermal iontophoretic drug delivery. Mechanistic analysis and application to polypeptide delivery. *J. Pharm. Sci.* **78**:370–375 (1989).
9. T. Kurihara-Bergstrom, K. Knutson, L. J. DeNoble, and C. Y. Goates. Percutaneous absorption enhancement of an ionic molecule by ethanol-water systems in human skin. *Pharm. Res.* **7**:762–766 (1990).
10. P. A. Cornwell and B. W. Barry. The routes of penetration of ions and 5-fluorouracil across human skin and the mechanisms of action of terpene skin penetration enhancers. *Int. J. Pharm.* **94**:189–194 (1993).
11. T. M. Tuvunen, S. Buyuktimkin, N. Buyuktimkin, A. Urtti, P. Paronen, and J. H. Rytting. Enhanced delivery of 5-fluorouracil through shed snake skin by two new transdermal penetration enhancers. *Int. J. Pharm.* **92**:89–95 (1993).
12. S. B. Ruddy and B. W. Hadzija. Iontophoretic permeability of polyethylene glycols through hairless rat skin: Application of hydrodynamic theory for hindered transport through liquid-filled pores. *Drug Design and Discovery* **8**:207–224 (1992).
13. S. M. Sims, W. I. Higuchi, and V. Srinivasan. Skin alteration and convective solvent flow effects during iontophoresis: I. Neutral solute transport across human skin. *Int. J. Pharm.* **69**:109–121 (1991).
14. J. C. Keister and G. B. Kasting. A kinetic model for ion transport across skin. *J. Membrane Sci.* **71**:257–271 (1992).
15. H. Inada, A. H. Ghanem, and W. I. Higuchi. Studies on the effects of applied voltage and duration on human epidermal membrane alteration/recovery and the resultant effects upon iontophoresis. *Pharm. Res.* **11**:687–697 (1994).
16. M. J. Pikal and S. Shah. Transport mechanisms in iontophoresis. III. An experimental study of the contributions of electroosmotic flow and permeability change in transport of low and high molecular weight solutes. *Pharm. Res.* **7**:222–229 (1990).
17. W. M. Deen. Hindered transport of large molecules in liquid-filled pores. *AIChE J.* **33**:1409–1425 (1987).
18. R. E. Beck and J. S. Schultz. Hindrance of solute diffusion within membranes as measured with microporous membranes of known pore geometry. *Biochim. Biophys. Acta* **255**:272–303 (1972).
19. R. A. Conradi, A. R. Hilgers, N. F. H. Ho, and P. S. Burton. The influence of peptide structure on transport across caco-2 cells. *Pharm. Res.* **8**:1453–1459 (1991).
20. T. Inamori, A. H. Ghanem, W. I. Higuchi, and V. Srinivasan. Macromolecular transport in and effective pore size of ethanol pretreated human epidermal membrane. *Int. J. Pharm.* **105**: 113–123 (1994).
21. W. M. Deen, M. P. Bohrer, and N. B. Epstein. Effect of molecular size and configuration on diffusion in microporous membranes. *AIChE J.* **27**:952–959 (1981).
22. K. D. Peck, A. H. Ghanem, W. I. Higuchi, and V. Srinivasan. Improved stability of the human epidermal membrane during successive permeability experiments. *Int. J. Pharm.* **98**:141–147 (1993).
23. P. Liu, J. A. S. Nightingale, and T. Kurihara-Bergstrom. Variation of human skin permeation in vitro: Ionic vs neutral compounds. *Int. J. Pharm.* **90**:171–176 (1993).
24. S. M. Sims, W. I. Higuchi, V. Srinivasan, and K. Peck. Ionic partition coefficients and electroosmotic flow in cylindrical pores: Comparison of the predictions of the Poisson-Boltzmann equation with experiment. *J. Colloid Interface Sci.* **155**:210–220 (1993).
25. V. A. Gierer and K. Wirtz. Molekulare theorie der mikroreibung. *Z. Naturforsch.* **8a**:532–538 (1953).
26. A. Leo, C. Hansch and D. Elkins. Partition coefficients and their uses. *Chem. Rev.* **71**:525–616 (1971).
27. W. D. Stein. *Transport and Diffusion Across Cell Membranes*, Academic Press, Orlando, 1986.
28. G. M. Golden, D. B. Guzek, A. H. Kennedy, J. E. Mckie, and R. O. Potts. Stratum corneum lipid phase transitions and water barrier properties. *Biochem.* **26**:2382–2388 (1986).
29. E. R. Scott, A. I. Laplaza, H. S. White, and J. B. Phipps. Transport of ionic species in skin: Contribution of pores to the overall skin conductance. *Pharm. Res.* **10**:1699–1709 (1993).
30. G. B. Kasting and L. A. Bowman. Electrical analysis of fresh, excised human skin: A comparison with frozen skin. *Pharm. Res.* **7**:1141–1146 (1990).